Simulation and Analyses of Staging Maneuvers of Next Generation Reusable Launch Vehicles

Bandu N. Pamadi[1], Thomas A. Neirynck[2], Peter F. Covell[3]
NASA Langley Research Center, Hampton, VA

Nathaniel Hotchko[4], David Bose[5]
Analytical Mechanics Associates, Inc., Hampton, VA

Abstract

NASA has initiated a comprehensive stage separation tool development activity to address the technology needed for successful development and operation of next generation reusable launch vehicles. As a part of this activity, ConSep simulation tool is being developed. This paper discusses the application of this tool to the staging maneuvers of two-stage-to-orbit (TSTO) vehicles. Simulation and analyses are performed for two bimese TSTO concepts, one staging at Mach 3 and the other at Mach 6. The TSTO bimese vehicles used in this study are sized for international space station class payload. The proximity and isolated aerodynamic databases used in the simulation were generated using the data from wind tunnel tests conducted at NASA Langley Research Center. ConSep is a MATLAB–based front end to the commercially available ADAMS solver, an industry standard package for solving multi-body dynamic problems.

Nomenclature

α	angle of attack, deg
$\Delta\alpha$	relative difference in angle of attack, deg
C_A, C_N,	axial and normal force coefficient
$C_{A,b}$, $C_{N,b}$	basic (isolated) axial and normal force coefficient
$C_{A,\text{int}}$, $C_{N,\text{int}}$	interference axial and normal force coefficients
$\Delta C_{A,\delta_e}$, $\Delta C_{N,\delta_e}$	axial and normal force coefficient increments due to elevon deflection
C_L, C_D	lift and drag coefficients
C_m	pitching moment coefficient
C_{mb}	basic (isolated) pitching moment coefficient
$\Delta C_{m,\text{int}}$	interference pitching moment coefficient
$C_{m,\delta e}$	pitching moment increment due to elevon deflection
Cmd	command
δ_e	elevon deflection, deg
γ	flight path angle, deg

---

[1] Aerospace Engineer, Vehicle Analysis Branch, Associate Fellow AIAA.
[2] Graduate Student, George Washington University
[3] Aerospace Engineer, Vehicle Analysis Branch, Senior Member AIAA.
[4] Project Engineer, Member AIAA.
[5] Supervising Engineer, Member AIAA.

h	altitude, ft
I_{xx}, I_{yy}, I_{zz}	moment of inertia about body x, y, z axis
k_1	stage separation interpolation constant
k_α, k_q	angle of attack and pitch rate feedback gains
L_{ref}	vehicle reference length, ft
M	Mach number
q	dynamic pressure, psf
V	velocity, ft/s
$\Delta x, \Delta z$	relative axial and normal distances during separation, ft
x_{cg}	x-location of center of gravity, ft
z_{cg}	z-location of center of gravity, ft

Introduction

NASA's Next Generation Launch Technology (NGLT) Program identified stage separation as one of the critical technologies needed for successful development and operation of NASA's next generation multistage reusable launch vehicles. As a step towards developing this critically needed technology, NASA has initiated a comprehensive stage separation tool development activity that includes wind tunnel testing, development and validation of CFD and engineering level tools. The reusable booster, a product of the NASA in-house small launcher[1] vehicle concept study, is used in a bimese configuration as the baseline in this tool development activity. This reusable booster concept is referred to as the Langley Glide-Back Booster[1] (LGBB). An overview of NASA's stage-separation tool development activity is presented in Ref. 2.

For a two-stage-to-orbit (TSTO) reusable launch vehicle (RLV), the staging Mach number depends on the design and operation of the vehicle. In this study, two vehicle concepts are considered, one which stages at Mach 3 with booster glide back to launch site and the other stages at Mach 6 with a booster that flies back to the launch site using air breathing jet engines. The two flight profiles are illustrated in Fig. 1. The objective of this paper is to demonstrate the application of the in-house engineering simulation tool called "ConSep" for the nominal staging of these two vehicle concepts. ConSep (previously named SepSim in Ref. 1) is being developed as a part of the NASA's stage separation tool development activity. The initial conditions for the staging maneuvers were assumed using the available ascent trajectories of similar vehicles. In this study, only the longitudinal motion of the booster and the orbiter are considered. The lateral/directional motion is not addressed.

Vehicle Description

The TSTO vehicles used in this study are bimese concepts. A TSTO vehicle in which both the booster and the orbiter have the same outer-mold-lines is called a bimese vehicle. In other words, external geometry of both the booster and orbiter are identical. For the bimese vehicles used in this study, the outer-mold-lines of both the booster and orbiter are identical to that the LGBB. However, the TSTO does not have the canards of the LGBB. Furthermore, both the bimese TSTO vehicles are approximately 4.16 times larger than LGBB in size. The LGBB vehicle is shown in Fig. 2 and a schematic arrangement of the belly-to-belly LGBB bimese configuration is presented in Fig. 3.

The sizing of the two bimese vehicles used in this study was based on Mach 3 Glideback and Mach 5 Flyback reference configurations developed during the NASA's ISAT (Intercenter Systems Analysis Team) effort which was part of the NGLT program. The reference mission assumed was to deliver a 35,000 lb payload to the ISS (International Space Station). For the purpose of this study, the SSME (Space Shuttle Main Engine) class engines are used on each stage. The ISAT Mach 3 configuration is very close to being considered a true "bimese" in that : 1). The outer mold lines are exactly the same, and 2). the internal arrangement is as similar as is practical, particularly in regards to tanks, primary structure and engines. Only the Orbiter has a reentry thermal protection system and payload provisions. The ISAT Mach 3 configuration uses fuel crossfeed from the booster to orbiter to maintain full orbiter fuel tanks at staging. The orbiter of the ISAT Mach 5 configuration was slightly smaller than the booster and hence not a true "bimese" configuration. The Mach 5 configuration booster uses 6 turbofan engines (20,000 lb thrust class) for flyback to the launch site, as the downrange was too great for glideback. These ISAT reference vehicles assume state–of-the-art technology in the design. Application of advanced technology would reduce the vehicle size, but this was not attempted in the present study.

The Mach 3 configuration of the present study is very similar in mass to the ISAT Mach 3 configuration. However, the Mach 6 configuration is a scaled up version of the Mach 5 ISAT configuration, and the orbiter grown even further to match the size of the booster. In order for this Mach 6 configuration to meet the mission requirements, the orbiter had to use some of its internal fuel prior to staging. Hence at separation, the orbiter's tanks are assumed to be less than full. Such an approach obviously leads to a suboptimal vehicle configuration but was required to match up the sizes of the booster and the orbiter to arrive at a true bimese TSTO configuration used in this study.

The schematic diagram of the attachment of the orbiter to the booster is shown in Fig. 4. The booster is attached to the orbiter at two points. Prior to the release, the forward joint is assumed to be a fixed support and the aft joint is assumed to permit rotation in pitch. These struts and the gap measurements are similar in geometry to the Shuttle Orbiter and External Tank attachment system except that the rear strut has a pivot linkage that allows the rotation of the booster relative to the upper stages upon release. This separation sequence is similar to that used in Ref. 3. The estimated mass properties of the two vehicles at staging are presented in Tables I and II.

Table I. Mass Properties at Staging for the Mach 3 Bimese TSTO Vehicle

Property	Orbiter	Booster
Weight, lbf	2,909,000	300,000
Total thrust	4,879,000	0
x_{cg}, ft	197.6	130.0
I_{xx}, slugs-ft^2	20,900,000	3,360,000
I_{yy}, slugs-ft^2	245,000,000	39,400,000
I_{zz}, slugs-ft^2	245,000,000	39,400,000

Table II. Mass Properties at Staging for the Mach 6 Bimese TSTO Vehicle

Property	Orbiter	Booster
Weight, lbf	2,230,000	476,000
Total thrust	4,899,000.0	0
x_{cg}, ft	197.6	130.0
I_{xx}, slugs-ft^2	16,000,000	5,330,000
I_{yy}, slugs-ft^2	188,000,000	62,600,000
I_{zz}, slugs-ft^2	188,000,000	62,600,000

American Institute of Aeronautics and Astronautics

Proximity Aerodynamic Characteristics and Development of Aerodynamic Database

The simulation and analyses performed in this study are limited to the stage separation events. The ascent and glideback/flyback trajectories are not addressed here. Two separate stage-separation databases were developed, one for the Mach 3 staging and the other for the Mach 6 staging. These two databases include the static longitudinal aerodynamic coefficients for proximity conditions and interference-free or isolated conditions. Theses databases do not include damping derivatives. The lateral/directional motion during stage separation is not addressed in this study.

The longitudinal stage-separation aerodynamic coefficients depend on the relative location of the two vehicles as characterized by three variables Δx, Δz and $\Delta\alpha$. A sketch showing the relative locations of the two vehicles during staging is shown in Fig. 5. The dependence of stage-separation aerodynamic coefficients on Δx, Δz and $\Delta\alpha$ is in addition to their usual dependence on Mach and α. Since the stage separation lasts only a few seconds, the Mach number is assumed to be constant during staging.

The proximity aerodynamic database was developed using the data from the stage separation wind tunnel tests conducted in the NASA Langley' s UPWT (Unitary Plan Wind Tunnel) at Mach 3 and the NASA Langley's 20-Inch Mach 6 Tunnel. Some Mach 3 stage separation tests were also conducted in the Aerodynamic Research Facility (ARF) at NASA's Marshall Space Flight Center (MSFC). The MSFC test data[4] was used as a reference but not in the development of the aerodynamic database discussed in this study. A brief description of the Langley's stage separation tests in UPWT and 20-Inch Mach 6 Tunnel is presented in this paper. Detail descriptions of the test facilities, support hardware, models, instrumentation and test procedure are available in Ref. 2. The incremental aerodynamic coefficients for the elevon deflections in proximity conditions were not available for either of the tests. In view of this, data from isolated model tests conducted on the LGBB model in the Langley UPWT (Mach range: 1.6 to 4.5) was used. Such data at Mach 6 was not available. The engineering level analysis tool APAS [5](Aerodynamic Preliminary Analysis System) was used to adjust the Mach 4.5 UPWT elevon deflection data for Mach 6 conditions.

The Mach 3 stage separation tests were conducted in the NASA Langley UPWT facility. The UPWT is a closed-circuit, continuous flow, pressure tunnel with two test sections that are nominally 4 ft by 4 ft in cross section and seven ft long. The Mach number range is 1.5 to 2.86 in Test Section I and 2.3 to 4.63 in Test Section II. Two LGBB 1.75% scale models were used. One LGBB model designated as the orbiter (bottom) model was always held at a fixed location and held fixed at $\alpha = 0$. The other test model designated as the booster (top) model was moved in x (aft) and in z (vertical) directions. All the x and z traverses were done for two values of angles of attack, 0 and 5 deg. The $\Delta x / L_{ref}$ and $\Delta z / L_{ref}$ range from 0 to 2.1 and 0 to 1.0 respectively. Thus, UPWT test data are available for $\Delta x / L_{ref}$ =0 to 2.1, $\Delta z / L_{ref}$ =0 to 1.0, at $\alpha = 0$, $\Delta\alpha = 0$ and $\alpha = 0$, $\Delta\alpha = 5$ deg. for the orbiter and for the booster at $\alpha = 0$, $\Delta\alpha = 0$ and $\alpha = 5$ deg, $\Delta\alpha = 5$ deg. A schematic illustration of the LGBB-bimese Mach 3 test matrix is presented in Fig.6.

The Mach 6 stage separation tests were conducted in the Langley 20-Inch Mach 6 Tunnel. Two 1.21% scale LGBB models were used, one as booster model and the other as orbiter model. All x movement was achieved by moving the booster (top) model aft of the orbiter (bottom) model. All z movement was achieved by lowering the orbiter model from the mated position. All x and z separations were run at $\Delta\alpha = 0$ and $\Delta\alpha = 5$ deg.. At each of the nominal x and z locations, both models were simultaneously swept through an angle of attack range of –10 degree to +10 degrees using the tunnel strut angle of attack mechanism so that α varied for each model whereas $\Delta\alpha$, Δx and Δz remain fixed at their nominal values. However, $\Delta\alpha = 5$ deg., the actual values Δx and Δz are slightly different due to the rotation in pitch from –10 deg to +10 deg.

The aerodynamic characteristics of booster and orbiter in proximity are significantly affected by the parameters $\Delta x, \Delta z$ and $\Delta\alpha$. To illustrate the physical nature of this interference, sample schlieren photographs[5] at Mach 3 conditions are presented in Fig. 8. In the mated condition ($\Delta x = \Delta z = \Delta\alpha = 0$), the mutual interference is characterized by a channel like flow between the two bodies and the bow shock waves of each body impinge on the other resulting in multiple reflections. As the two bodies move short distance apart in x and z directions, the channel like

flow is not observed. Instead, the mutual interference is mainly determined by bow shock impingements and their reflections. It is interesting to note that the orbiter falls out of booster's influence much earlier than the booster going out of orbiter's influence. For example, for $\Delta x = 0.4, \Delta z = 0.25$, the orbiter is nearly out of booster's influence whereas the booster is still under the orbiter's influence. The shock intersections affect the pressure distribution causing it to rise over the downstream part of the body resulting in significant variations particularly in the normal and pitching moment coefficients. The flow pattern over the LGBB-bimese models at Mach 6 has similar features but differs from the Mach 3 because the shock angles are much steeper.

The isolated aerodynamic coefficients at Mach 3 and Mach 6 are presented in Fig. 9. To illustrate the physical nature of variation of longitudinal aerodynamic coefficients in the proximity environment, selected wind tunnel test data are presented in Figs. 10-17. In Figs. 10-15, the total coefficients are presented for Mach 3 case. However, the test data for Mach 6 was in the form of incremental coefficients with respect to the corresponding isolated condition and these incremental coefficients are presented in Figs. 16 and 17. It can be observed from these figures that both at Mach 3 and 6, the vehicles would move apart if released from mated condition ($\Delta x = \Delta z = \Delta \alpha = 0$) because they experience positive normal force coefficients and pitching moment coefficients which aid the staging process. If it were the opposite of this, that is, a negative normal force and a negative pitching moment coefficient, then the two bodies would tend to move towards each other and result in a re-contact.

Both the Langley Mach 3 and Mach 6 proximity test data do not cover sufficiently large values of Δx and Δz so that the test data transition smoothly from stage separation (proximity) type to isolated (interference free) data. This aspect is particularly true for the booster. In view of this, following assumption was introduced to transition smoothly from the available stage-separation aero data to the isolated aero data for each vehicle as they move apart. For zero control deflection,

$$C_A = k_1 C_{A,b} + (1 - k_1)C_{A,\text{int}}$$

$$C_N = k_1 C_{N,b} + (1 - k_1)C_{N,\text{int}}$$

$$C_m = k_1 C_{m,b} + (1 - k_1)C_{m,\text{int}}$$

Here, C_A, C_N and C_m, denote the axial force, normal force and pitching moment coefficients in staging environment, $C_{A,b}$, $C_{N,b}$ and $C_{m,b}$ are basic or isolated axial force, normal force and pitching moment coefficients, $C_{A,\text{int}}$, $C_{N,\text{int}}$ and $C_{m,\text{int}}$ are the stage-separation or the proximity aerodynamic coefficients, k_1 is an interpolation constant for transition from the stage-separation aerodynamics ($k_1 = 0$) to the basic (isolated) aerodynamics ($k_1 = 1$). The transition region is assumed to consist of an inner ellipse and an outer ellipse which are defined empirically using the stage separation test data as guide. Both the ellipses are assumed to be centered at the moment reference point of each model. The parameter k_1 is assumed to vary linearly from 0 at the inner ellipse to 1 at the outer ellipse. The control surface increments like $\Delta C_{A,\delta e}$ due to elevons , when used, were added to the above coefficients.

Simulation of Staging Maneuvers

The simulation of staging maneuvers was done using the in-house software tool called ConSep (previously called SepSim in Ref.1). The ConSep is a MATLAB-based front end to the commercially available ADAMS[7] solver, an industry standard package for solving multi-body dynamic problems. ConSep is configured for the simulation of TSTO staging maneuvers. It has the capability to model multiple joints, separation forces due to reaction jets or piston type devices, closed-loop proportional and derivative (PD) control, actuator dynamics, atmospheric winds, engine gimbals, engine plumes etc. It is also configured for Monte Carlo studies. Additional information on ConSep is available in Ref. 7.

The following initial conditions were used for the simulation of staging events: (i) Mach 3 Staging: Altitude = 85000.0 ft, Velocity = 2921.6 ft/sec, dynamic pressure (q) = 300 lb/sft, flight path angle (γ) = 53.0 deg, α (booster) =0 and α (orbiter) = 0, (ii) Mach 6 Staging: Altitude 150,000 ft, Velocity= 6586.8 ft/sec, dynamic pressure (q)= 75 lbs/sft, flight path angle (γ) = 53.0, deg., α (booster) =0 and α (orbiter) = 0.

The Synergistic Engineering Environment (SEE) environment was used to create animations of the staging maneuvers. The SEE used the geometry models of the LGBB and the ConSep output to generate these animations. The geometrical shape of the orbiter engine plume was assumed to be a cylinder of constant diameter equal to base diameter because the exit plume was nearly over expanded for both Mach 3 and Mach 6 staging conditions. The SEE animation provides an effective means for collision detection or engine plume interactions. Additional information on SEE is available in Ref. 8.

Results and Discussion

In the present study, only aerodynamic separation assisted with thrust gimbaling was attempted. Separation forces or thrusters were not used. At staging, the angle of attack of each vehicle was assumed to be zero, the orbiter thrusting and the booster with zero thrust. The staging event starts with the release of the forward joint at about t=0.05 sec permitting the booster to rotate about the aft joint. For both Mach 3 and Mach 6 staging, the booster's angle of attack steadily increases partly due to the positive normal force and positive pitching moment coefficients in proximity and partly due to the pulling action by the thrusting orbiter. For Mach 3 staging at 85000 ft, the dynamic pressure is around 300 lb/sft and for Mach 6 staging, its value is around 75 lbs/sft. Thus, the aerodynamic forces and moments acting on the vehicles at Mach 3 are approximately four times higher compared to the Mach 6 staging case.

For Mach 3 staging, the aft joint was released at t=0.1 sec, thus releasing the booster. The trajectory variables for Mach 3 staging are presented in Figs. 18 and 19. Some snap shots from the SEE animation at selected time intervals are presented in Fig. 20. In these figures, the booster is designated as vehicle 1 and the orbiter as vehicle 2. It was observed that a simple passive release of the booster with no active closed-loop feedback control (baseline) causes the orbiter's angle of attack to steadily decrease and become negative making the orbiter's nose to turn toward the booster. Even though the two vehicles may be appearing to move away from each other as indicated by the increasing values of Δx and Δz, the two vehicles may not be that far apart due to the decreasing value of angle of attack of the orbiter. With active control using elevons for each vehicle, the situation improves considerably (Figs. 21 and 22). The schematic diagram of the PD (Proportional plus Derivative) controller implemented in ConSep is shown in Fig.23. The feedback gains were adjusted by trial and error as $k_\alpha = 0, k_q = -0.4$ for the booster and $k_\alpha = -4.0, k_q = 1.0$ for the orbiter. The commanded angle of attack (α_{cmd}) for the booster was 5 deg and zero for the orbiter. With feedback control, the orbiter's angle of attack stays close to zero but the booster's angle of attack overshoots above 5 deg and continues to oscillate. However, it was observed that by about 3.0 seconds, relative to the orbiter, the booster is about 200 ft and 120 ft above. Continuing the simulation beyond 3 sec indicated that the two vehicles continue to move apart. Hence, at this point, the stage separation can be assumed to be safely completed and each vehicle can be flown on its designated flight trajectory.

Since the booster's angle of attack goes beyond 5 deg with $\Delta\alpha$ exceeding 5 deg, the simulation tends to go out of range of the proximity database which is not desirable. To prevent this from happening and in the absence of better alternatives, the extrapolation was not permitted in the use of aero database. In other words, the values of aero coefficients were held frozen at those corresponding to $\alpha = \Delta\alpha = 5$ deg. This is certainly not satisfactory but it is a limitation in the proximity database and not that of ConSep. Further, the use of pitch rate feedback during staging indicates that the dynamic or damping derivatives need to be evaluated and included in the proximity and isolated aero databases.

The results of simulation for Mach 6 staging are presented in Figs. 24-28. For this case, simple aerodynamic separation with no thrust vectoring (baseline) does not appear to be satisfactory because the aerodynamic forces are small due to reduced dynamic pressure. This problem is particularly severe for the orbiter because it is much heavier in mass and pitch inertia. With no active feedback control, the angle of attack of the orbiter steadily decreases and goes negative. As said before, this causes the nose of the orbiter to turn towards the booster and that is not desirable. Using controls (elevons) deflected to their expected limits right from the beginning on both vehicles was not of much help because the incremental aerodynamic forces and moments are small. However, it so happens that when the orbiter's nose turns towards the booster, its tail turns away which is helpful to avoid booster contact with the orbiter's engine plume. Thus, a small and steady negative value of angle of attack of the orbiter is beneficial. For this purpose, the orbiter's thrust gimbaling by a small amount proved to be helpful. The results presented in Figs. 26-27 are based on using a -0.125 deg (up) gimbaling of orbiter's engines. This helps to keep the orbiter's

pitch rate close to zero and stabilize its angle of attack around –2 deg. By about 3.0 seconds, the booster has moved aft and above the orbiter. The selected snap shots for this case are presented in Fig. 28. These separation distances are much smaller than the Mach 3 case and are indicative of the problems associated with Mach 6 staging. However, these observations are preliminary in nature considering the fact that the proximity aerodynamic database does not cover the complete range of separation distances and angles of attack values encountered in the present simulations.

Concluding Remarks

The analyses and simulation of the staging maneuvers of two TSTO vehicle concepts, one staging at Mach 3 and the other staging Mach 6 were performed to demonstrate the application of the in-house developed ConSep tool. ConSep is being developed as a part of NASA's stage separation tool development activity for developing the technologies needed for successful design, development and operation of next generation reusable multi-stage launch vehicles. The TSTO vehicles used in this study were bimese concepts with outer-mold-lines identical to that of the Langley Glide-Back Booster (LGBB) that was used as the baseline vehicle in NASA's stage separation tool development activity. The proximity aerodynamic databases were developed using the available data from stage separation wind tunnel tests conducted at NASA Langley Research Center. The simulation results coupled with animation/visualization capability provide a valuable tool for analysis and simulation of staging maneuvers of next generation reusable launch vehicles.

References

1) Pamadi, B.N., Tartabini, P.V., and Starr, B.R.; Ascent, Stage Separation and Glideback Performance of a Partially Reusable Small Launch Vehicle, AIAA Paper 2004-0876.

2) Murphy, K.J., Buning, P.G., Pamadi, B.N., Scallion, W.I., and Jones, K.M.; Status of Stage Separation Tool Development for Next Generation Launch Vehicle Technologies. Paper to be presented at the 24th AIAA Aerodynamic Measurement Technology and Ground Testing, Portland, Or, June 2004.

3) Naftel, J.C., Powell, R.W., *Analysis of the Staging Maneuver and Booster Glideback Guidance for a Two-Stage, Winged, Fully Reusable Launch Vehicle*, NASA TP 3335, 1993.

4) Bordelon, W.J., Frost, A.L., Reed, D.K., Stage Separation Wind Tunnel tests of a Generic Two-Stage-to-Orbit Launch Vehicle, AIAA Paper 2003-4227, July 2003.

5) Bonner, E., Clever, E., and Dunn, K., *Aerodynamic Preliminary Analysis System II, Part I – Theory*, NASA CR 182076, April 1991.

6) *Using ADAMS/Solver*, Mechanical Dynamics, Inc., 1999.

7) Bose D.M., and Hotchko, N., Conceptual Level *Stage Separation Simulation (ConSep)–Version 1.1 User's Guide*, AMA Report No. 02-37 Rev.B, Analytical Mechanics Associates, Hampton, VA, December 2003.

8) Angster, S., *Synergistic Engineering Environment Build II User's Guide Revision E*, AMA Report No. 03-31, Analytical Mechanics Associates, Hampton, VA, August 2003.
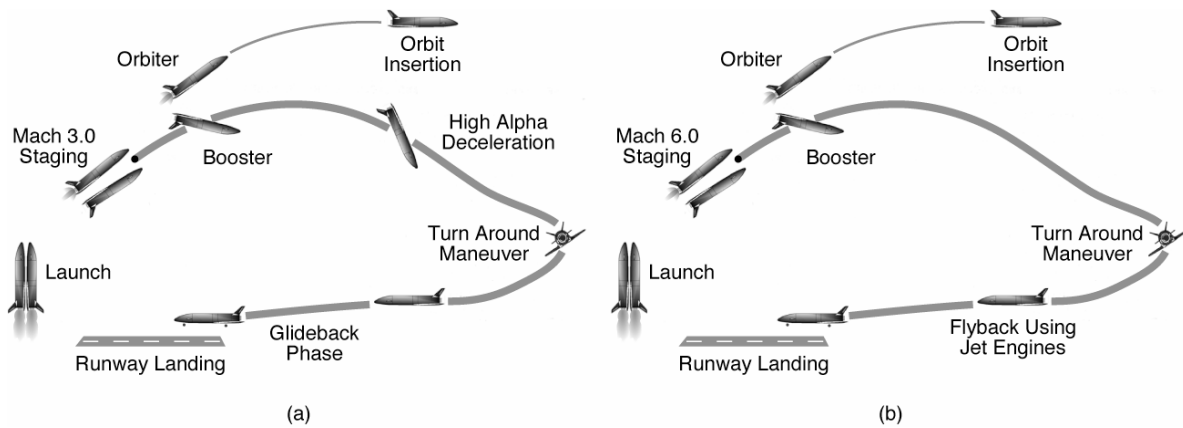
Figure 1. Illustration of the flight profiles.
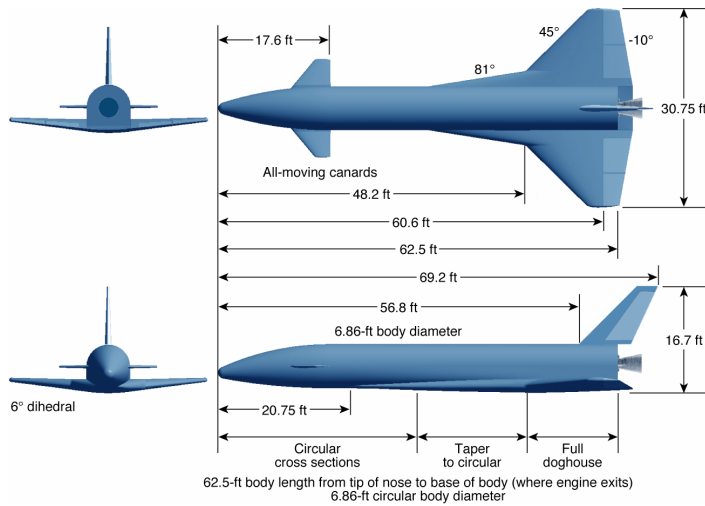
Figure 2. Three-view diagram of the Langley glide-back booster (LGBB).
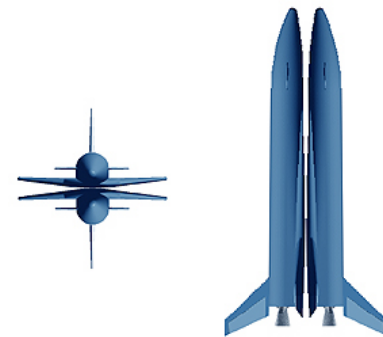
Figure 3. Bimese version of the LGBB TSTO Vehicle.
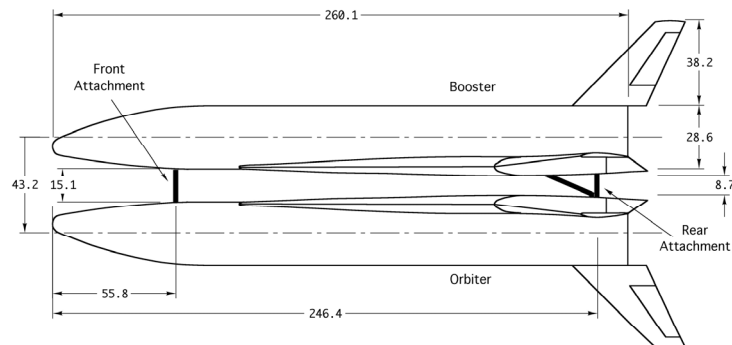
Figure 4. Schematic illustration of the attachment of the booster and the orbiter.

8

American Institute of Aeronautics and Astronautics
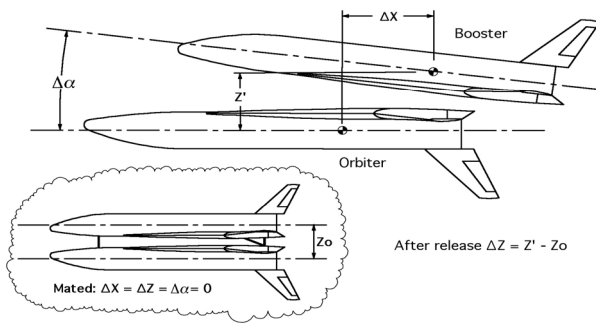
Figure 5. Relative locations of vehicles during stage separation.
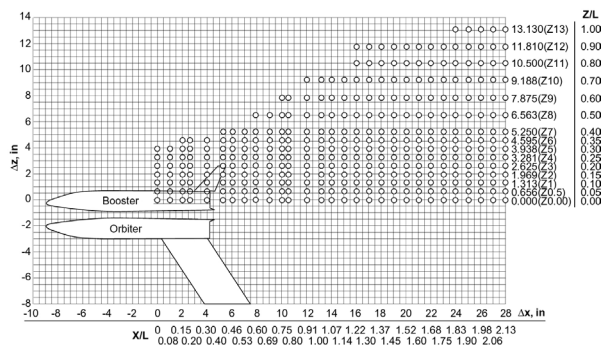
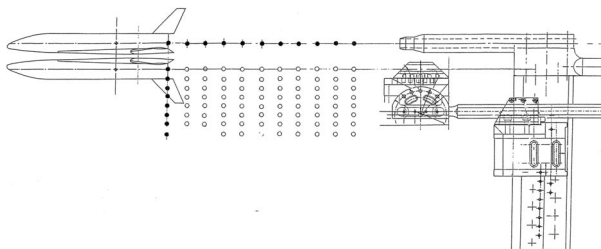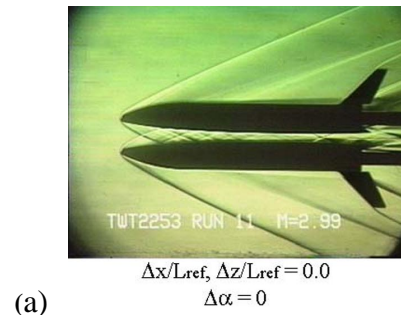**Figure 6. Schematic illustration of LGBB-Beimese UPWT test matrix at Mach 3.**

Figure 7. Schematic illustration of the LGBB-Bimese Mach 6 Tunnel test matrix.

(a)
$\Delta x/L_{ref}, \Delta z/L_{ref} = 0.0$
$\Delta \alpha = 0$

(b)
$\Delta x/L_{ref} = 0.2, \Delta z/L_{ref} = 0.16$
$\Delta \alpha = 5$

(c)
$\Delta x/L_{ref} = 0.4, \Delta z/L_{ref} = 0.25$
$\Delta \alpha = 5$

(d)
$\Delta x/L_{ref} = 0.8, \Delta z/L_{ref} = 0.36$
$\Delta \alpha = 5$
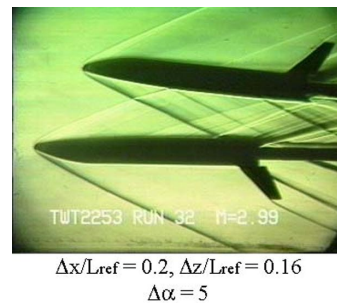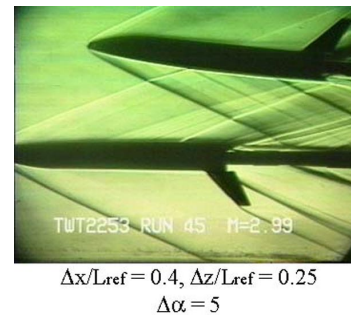
Figure 8. Schlieren Photographs of the LGBB bimese configurations at Mach 3 stage-separation environement in MSFC Aerodynamic Research Facility[4].

American Institute of Aeronautics and Astronautics
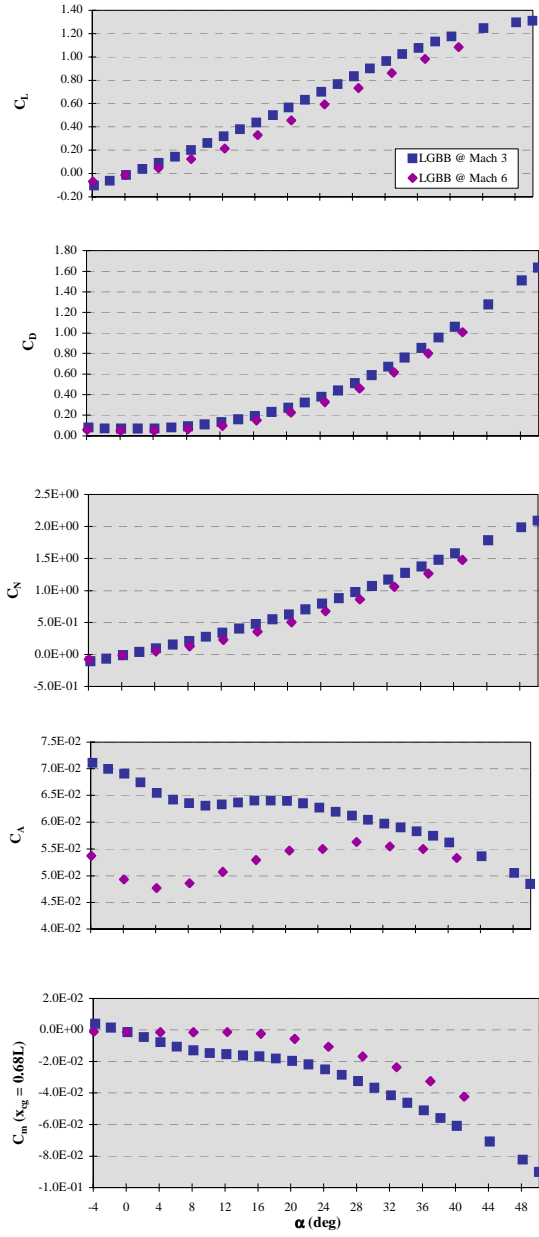
Figure 9: Variation of Isolated LGBB lift, drag, normal and axial force, and pitching moment coefficient with AoA at Mach 3 and 6.
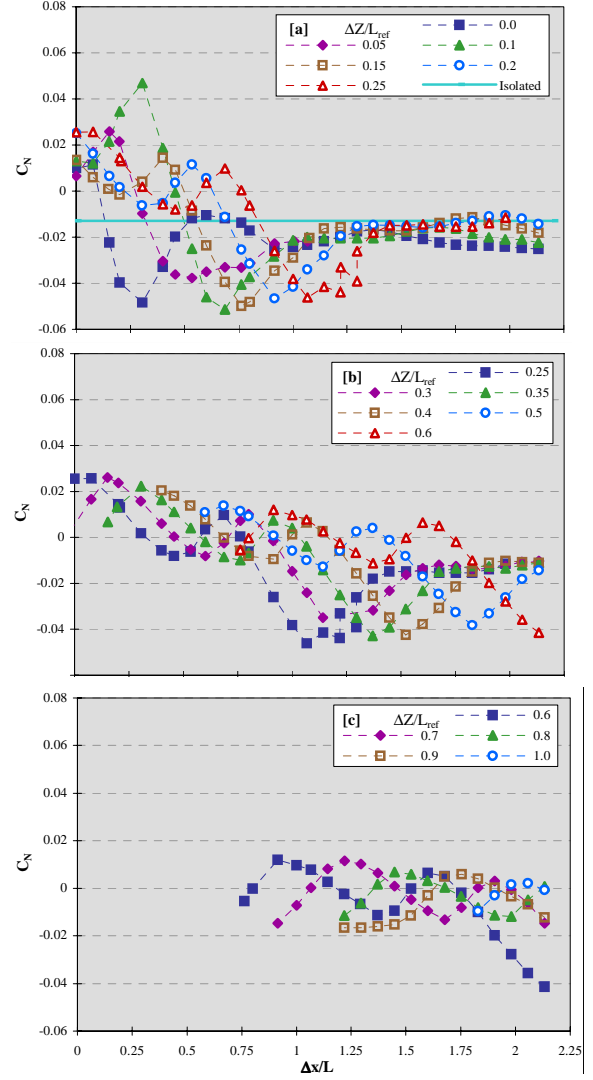
Figure 10: Variation of bimese-booster normal force coefficient with $\Delta x/L_{ref}$ and $\Delta z/L_{ref}$ at Mach 3 for $\alpha = 0$, $\Delta\alpha = 0$ degrees.
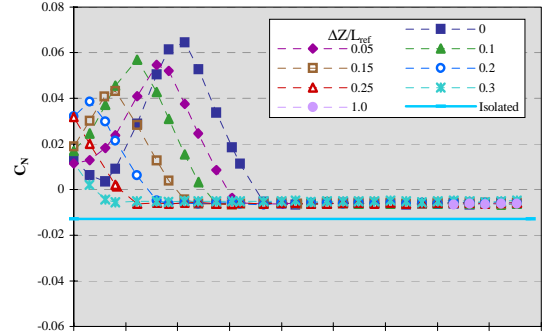

Figure 11: Variation of bimese-orbiter static normal force coefficient with $\Delta x/L_{ref}$ and $\Delta z/L_{ref}$ at Mach 3 for $\alpha = 0$, $\Delta\alpha = 0$ degrees.
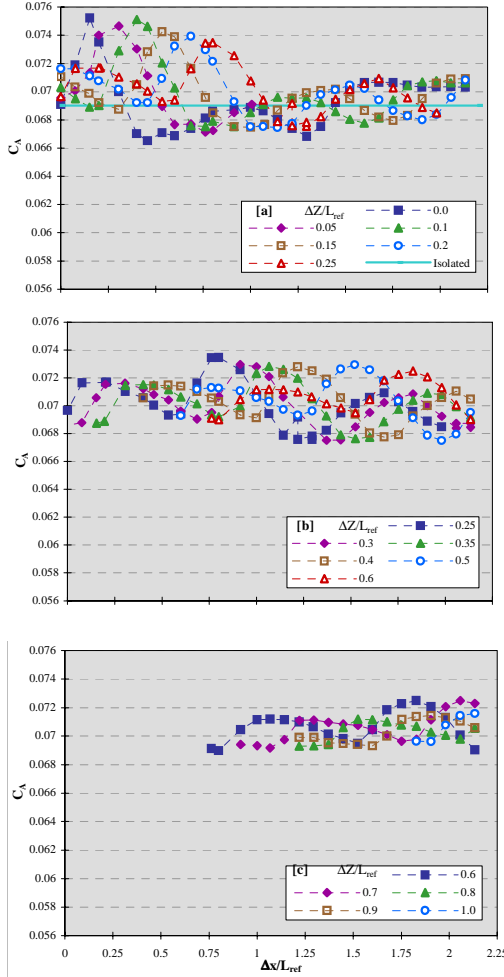
Figure 12: Variation of bimese-booster axial force coefficient with $\Delta x/L_{ref}$ and $\Delta z/L_{ref}$ at Mach 3 for $\alpha = 0$, $\Delta\alpha = 0$ degrees.
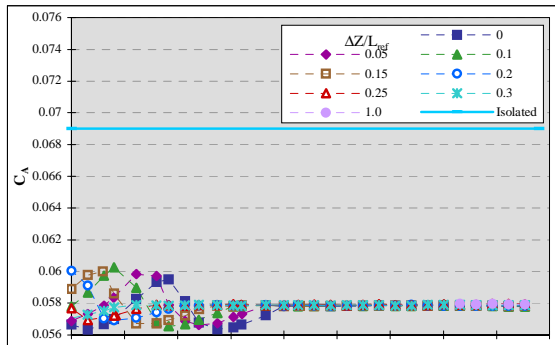
Figure 13: Variation of bimese-orbiter axial force coefficient with $\Delta x/L_{ref}$ and $\Delta z/L_{ref}$ at Mach 3 for $\alpha = 0$, $\Delta\alpha = 0$ degrees.
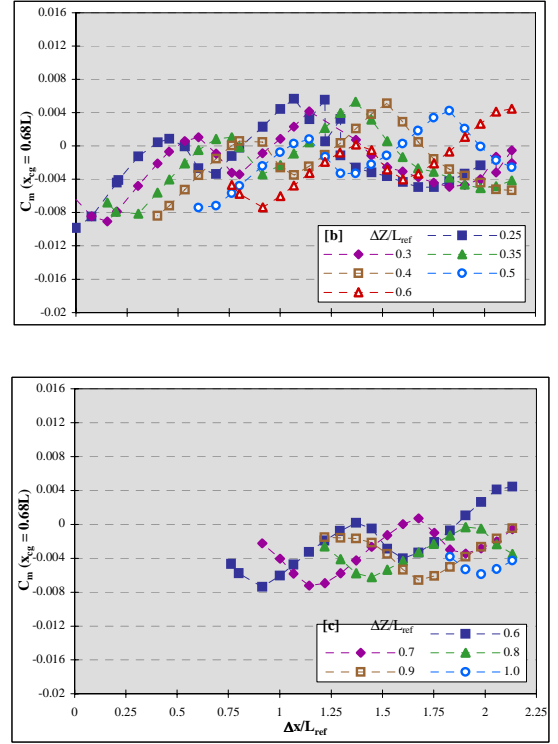
Figure 14: Variation of bimese-booster pitching moment coefficient with $\Delta x/L_{ref}$ and $\Delta z/L_{ref}$ at Mach 3 for $\alpha = 0$, $\Delta\alpha = 0$ degrees.
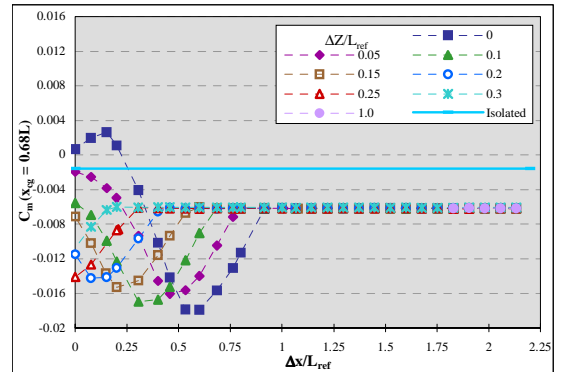
Figure 15: Variation of bimese-orbiter pitching moment coefficient with $\Delta x/L_{ref}$ and $\Delta z/L_{ref}$ at Mach 3 for $\alpha = 0$, $\Delta\alpha = 0$ degrees.

American Institute of Aeronautics and Astronautics

Figure 16. Proximity aerodynamic coefficients for Mach 6 at $\alpha = 0$ **and** $\Delta\alpha = 0$**.**

Figure 17. Proximity aerodynamic coefficients at Mach 6, $\Delta\alpha = 5.0$.
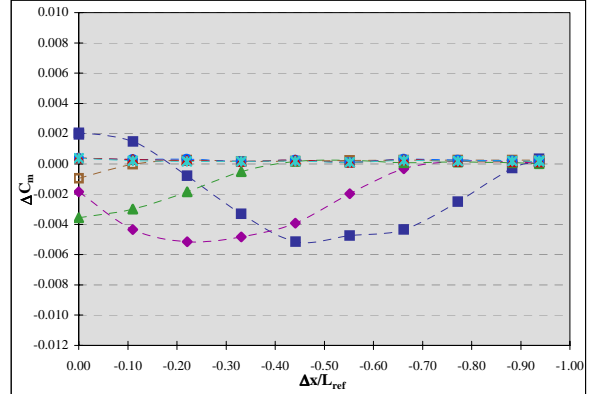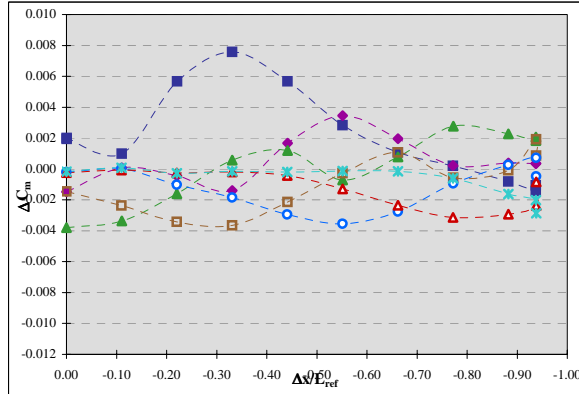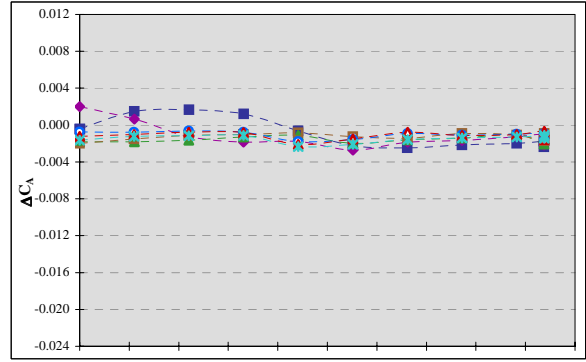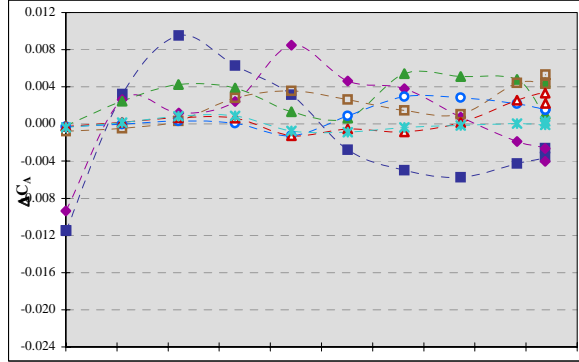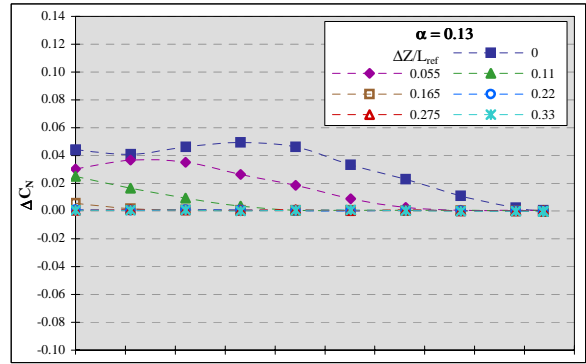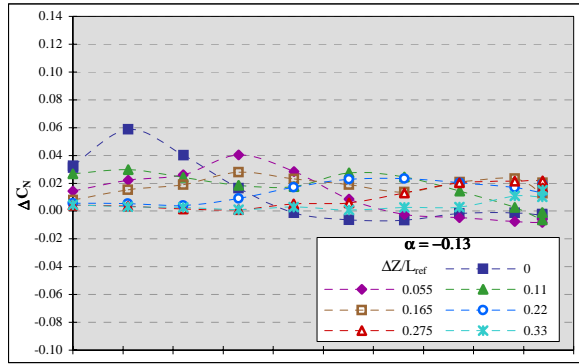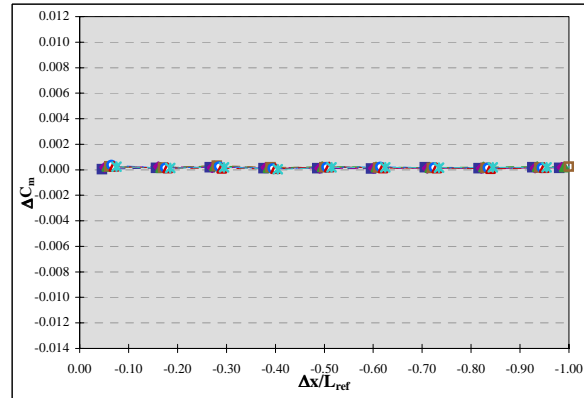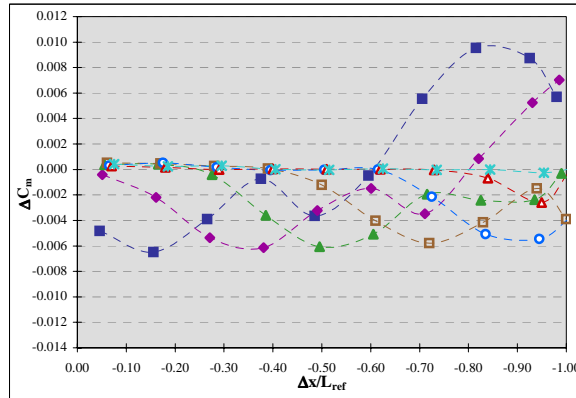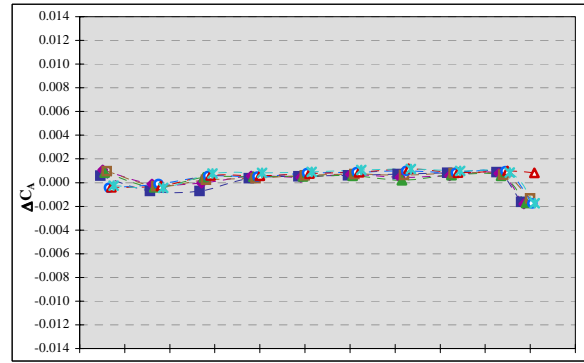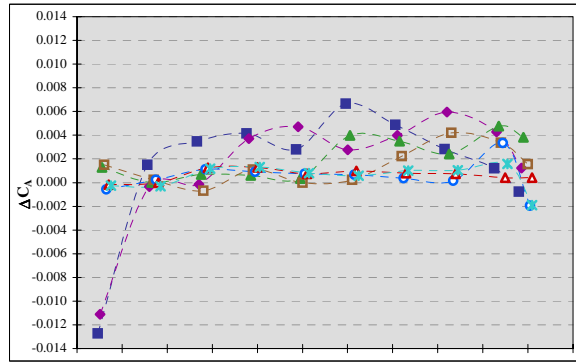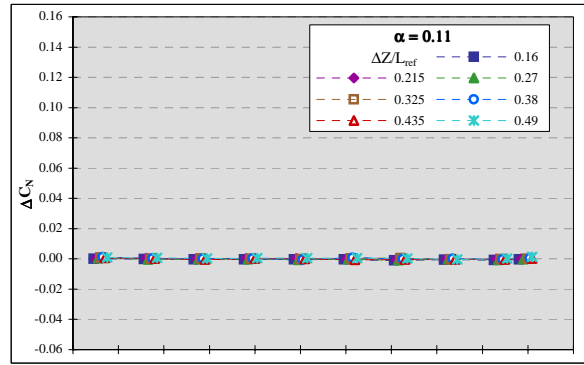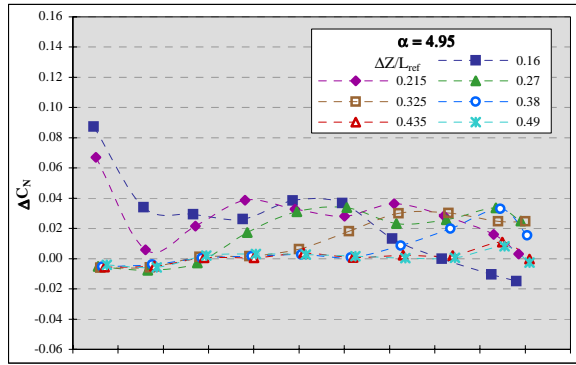
Vehicle 1 (Booster) @ $\Delta\alpha = 5$ degrees

Vehicle 2 (Orbiter) @ $\Delta\alpha = 5$ degrees

American Institute of Aeronautics and Astronautics
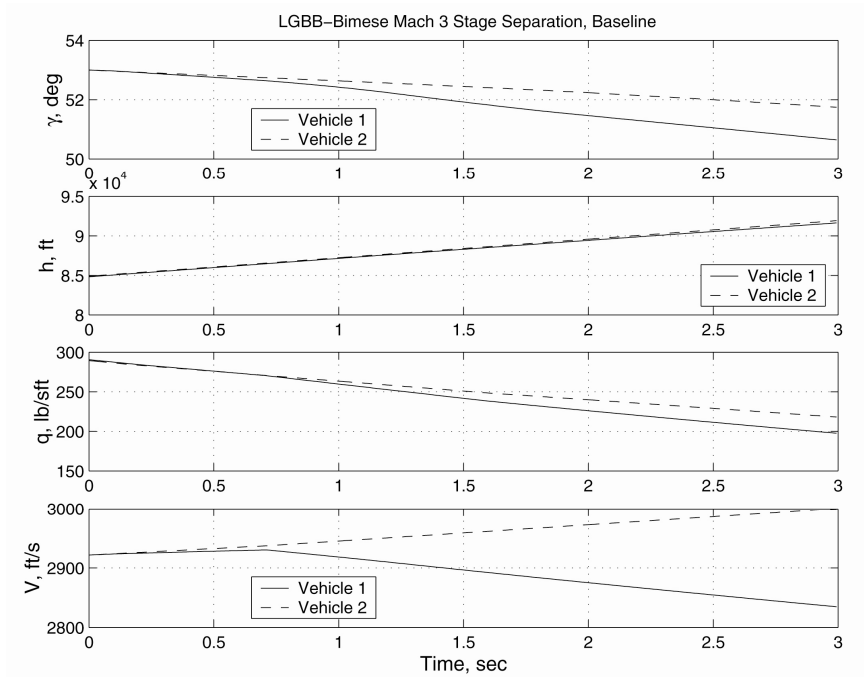
Figure 18. Variation of flight path angle (γ), altitude (h), dynamic pressure (q) and velocity (V) for baseline Mach 3 stage separation.
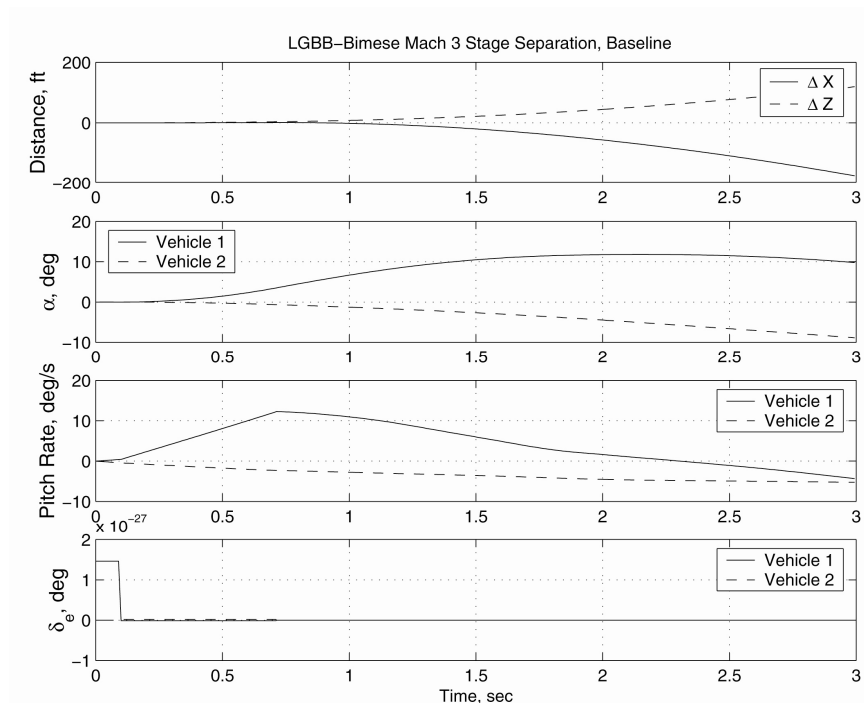
Figure 19. Variation of separation distances, angle of attack (α), pitch rate and elevon deflections during baseline Mach 3 stage separation.
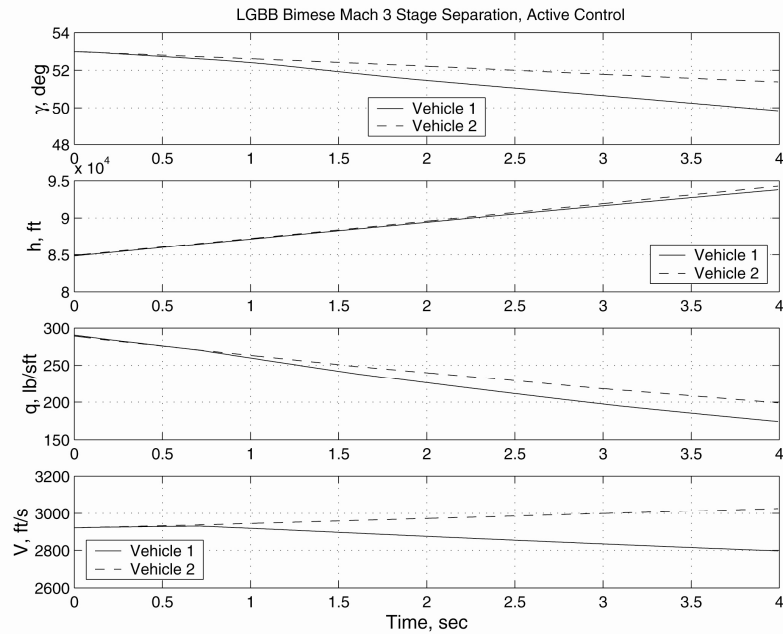
14

Figure 20. Variation of flight path angle (γ), altitude (h), dynamic pressure (q) and velocity (V) for Mach 3 stage separation with active control.
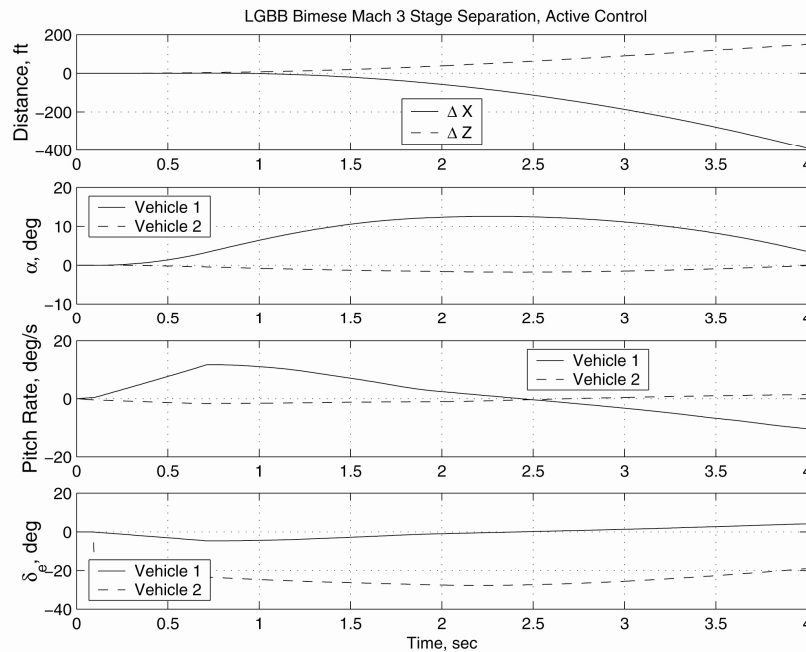

Figure 21. Variation of separation distances, angle of attack (α), pitch rate and elevon deflections during Mach 3 stage separation with active control.

American Institute of Aeronautics and Astronautics

(a) t=0, Mated Configuration

(d) t=2.0 sec.

(b) t=0.5 sec, Aft Joint Release.

(e) t=2.5 sec.
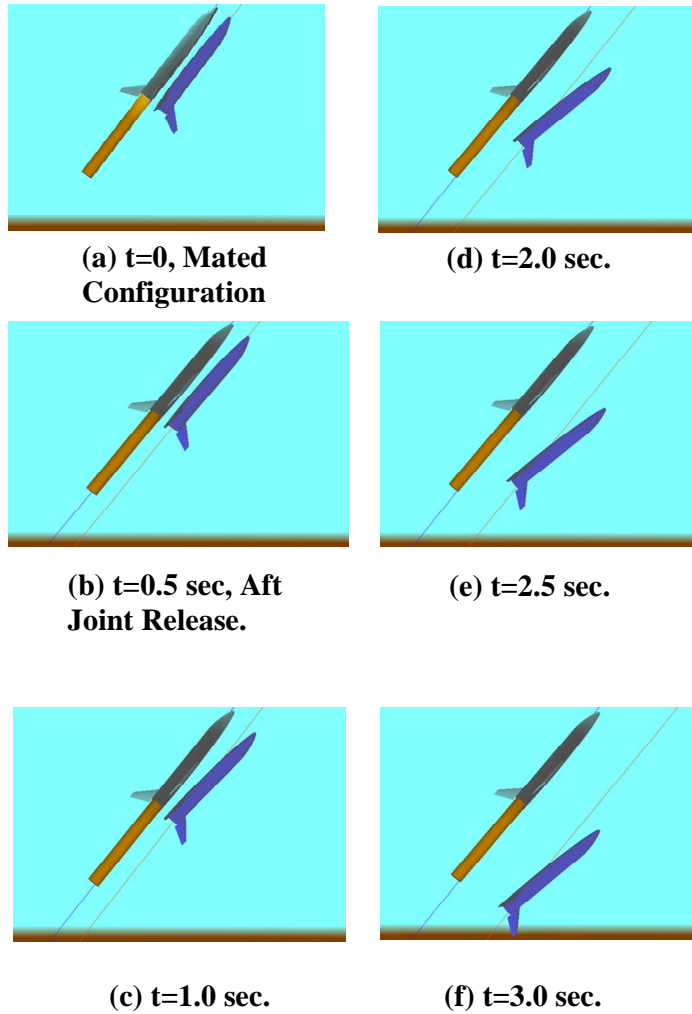

(c) t=1.0 sec.

(f) t=3.0 sec.

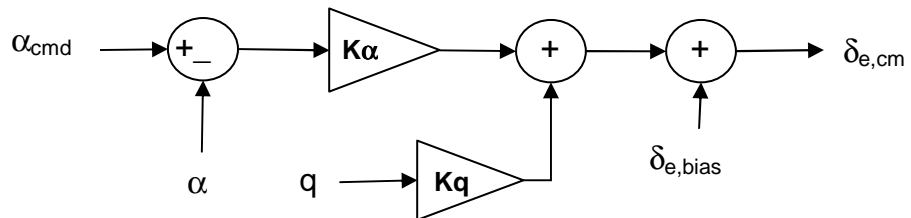**Figure 22. Relative location of vehicle during Mach 3 stage separation with active control.**

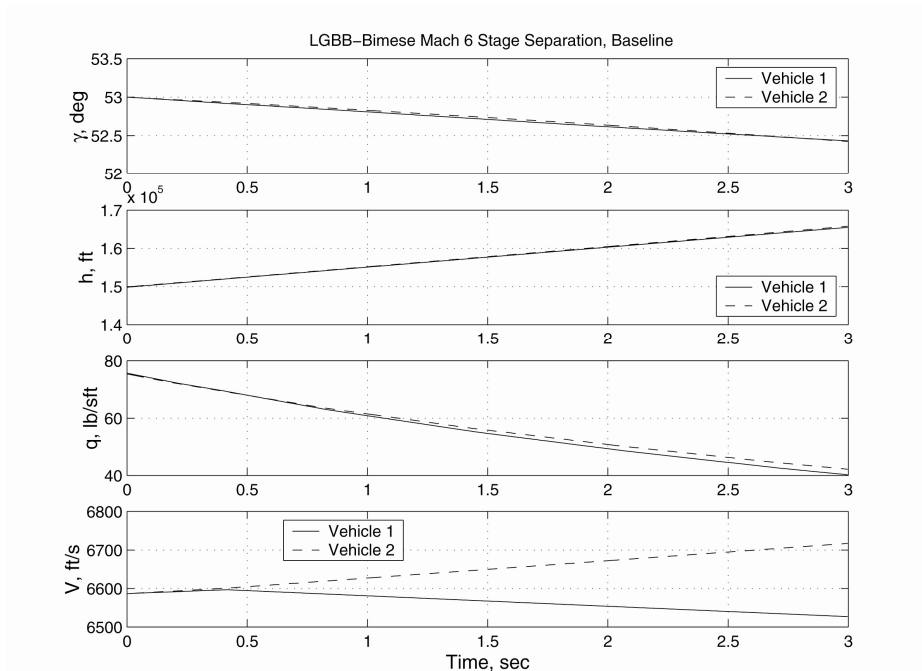
**Figure 23. Feedback control system
implemented in ConSep.**

Figure 24. Variation of flight path angle (γ), altitude (h), dynamic pressure (q)and velocity (V) for baseline Mach 6 stage separation.
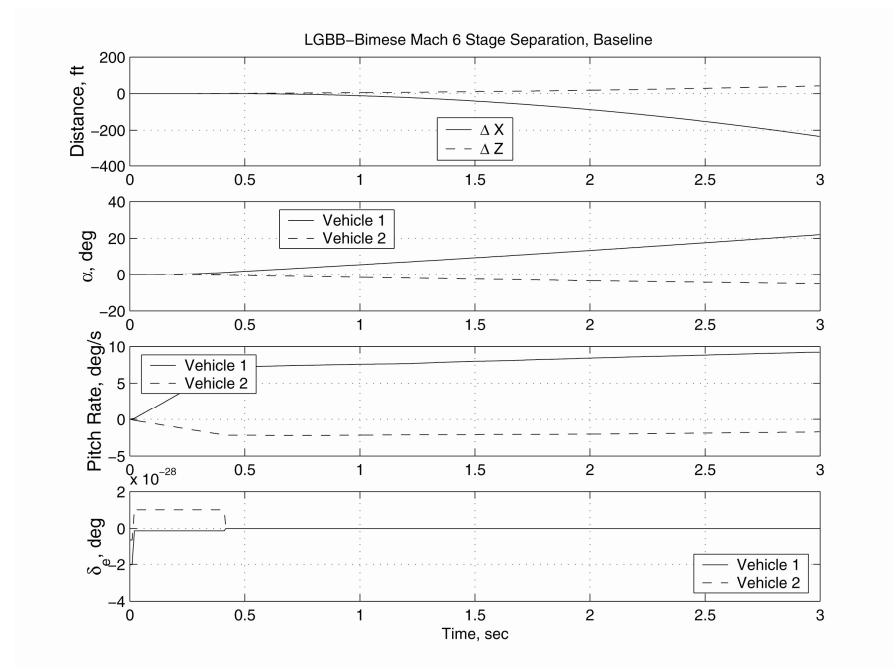

Figure 25 Variation of separation distances, angle of attack (α), pitch rate and elevon deflections during baseline Mach 3 stage separation.

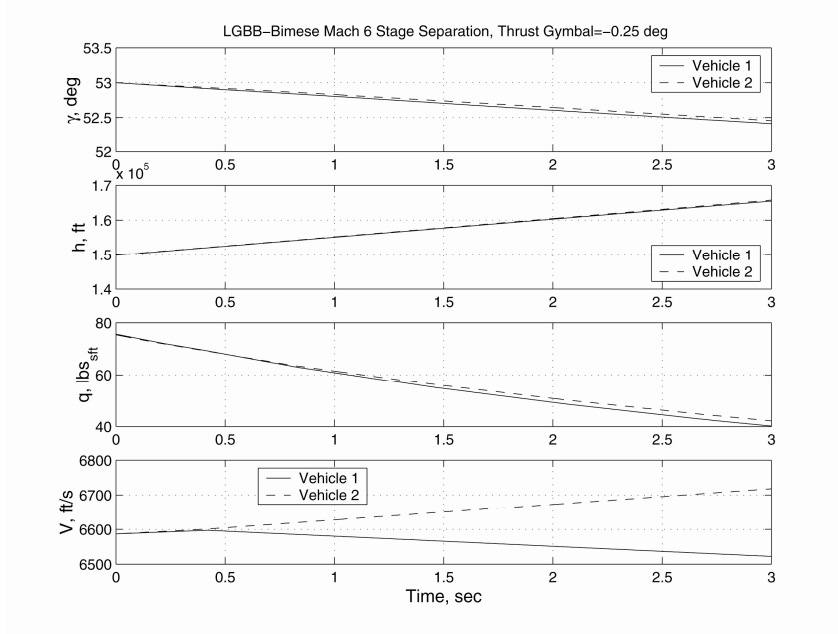American Institute of Aeronautics and Astronautics

Figure 26. Variation of flight path angle (γ), altitude (h), dynamic pressure (q) and velocity (V) for Mach 6 stage separation with engine gimbal control.
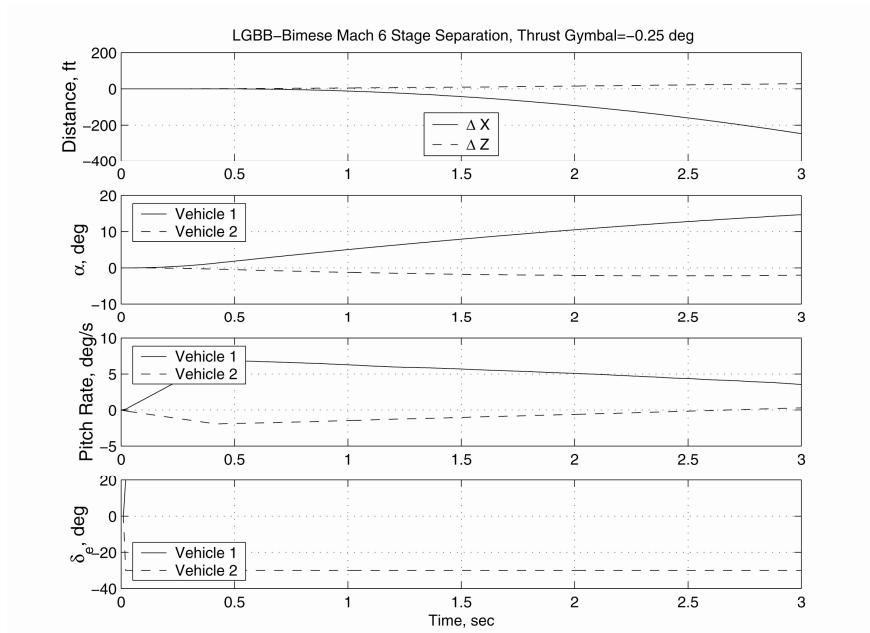

Figure 27. Variation of separation distances, angle of attack (α), pitch rate and elevon deflection (δ_e) during Mach 6 stage separation with engine gimbal control.

American Institute of Aeronautics and Astronautics

(a) t=0, Mated Configuration.

(b) t=0.5 sec, Aft Joint Release.

(c) t=1.0 sec.
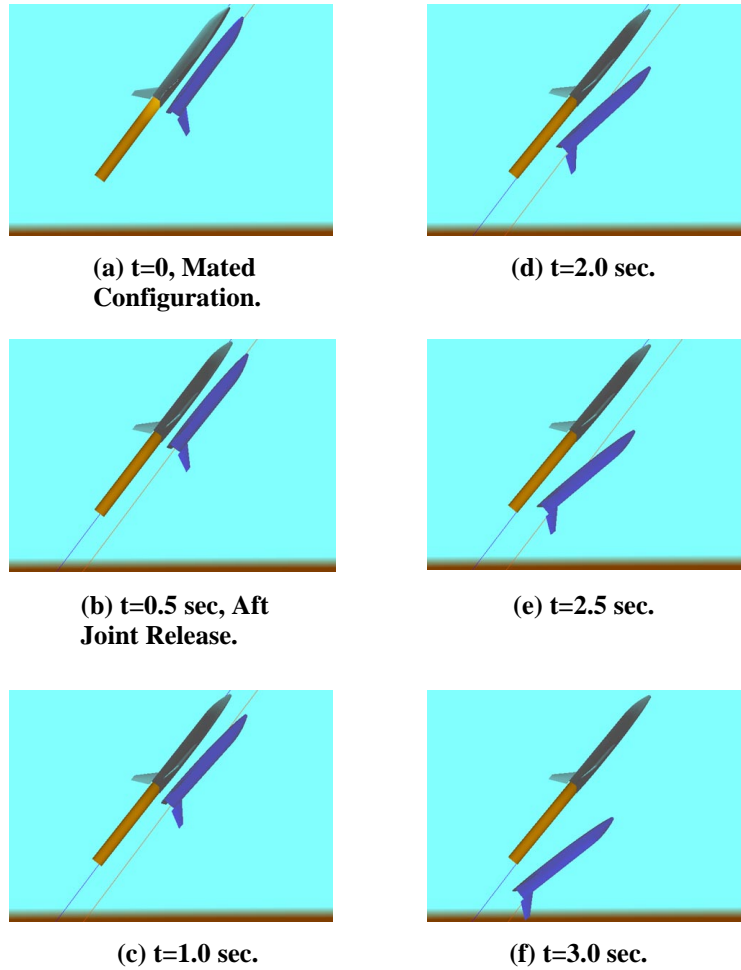
(d) t=2.0 sec.

(e) t=2.5 sec.

(f) t=3.0 sec.

Figure 28. Relative location of vehicle during Mach 6 stage separation with gimbal angle control.

American Institute of Aeronautics and Astronautics